Ecosystems (2007) 10: 1100–1115
DOI: 10.1007/s10021-007-9079-y

ECOSYSTEMS

Intraseasonal Variation in Water and Carbon Dioxide Flux Components in a Semiarid Riparian Woodland

Enrico A. Yepez,[1,4,*] Russell L. Scott,[2] William L. Cable,[2,3] and David G. Williams[3]

[1]*School of Natural Resources, University of Arizona, Tucson, Arizona 85721, USA;* [2]*Southwest Watershed Research Center, USDA, Agricultural Research Service, Tucson, Arizona 85719, USA;* [3]*Department of Renewable Resources and Botany, University of Wyoming, Laramie, Wyoming 82071, USA;* [4]*Department of Biology, University of New Mexico, Castetter Hall Room 167, Albuquerque, New Mexico 87131, USA*

Abstract

We investigated how the distribution of precipitation over a growing season influences the coupling of carbon and water cycle components in a semiarid floodplain woodland dominated by the deep-rooted velvet mesquite (*Prosopis velutina*). Gross ecosystem production (GEP) and ecosystem respiration (R_{eco}) were frequently uncoupled because of their different sensitivities to growing season rainfall. Soon after the first monsoon rains, R_{eco} was high and was not proportional to slight increases in GEP. During the wettest month of the growing season (July), the system experienced a net carbon loss equivalent to 46% of the carbon accumulated over the 6-month study period (114 g C m^{-2}; May–October). It appears that a large CO_2 efflux and a rapid water loss following precipitation early in the growing season and a later CO_2 gain is a defining characteristic of seasonally dry ecosystems. The relative contribution of plant transpiration (T) to total evapotranspiration (ET) (T/ET) was 0.90 for the entire growing season, with T/ET reaching a value of 1 during dry conditions and dropping to as low as 0.65 when the soil surface was wet. The evaporation fraction (E) was equivalent to 31% of the precipitation received during the study period (253 mm) whereas trees and understory vegetation transpired 38 and 31%, respectively, of this water source. The water-use efficiency of the vegetation (GEP/T) was higher later in the growing season when the C4 grassy understory was fully developed. The influence of rain on net ecosystem production (NEP) can be interpreted as the proportion of precipitation that is transpired by the plant community; the water-use efficiency of the vegetation and the precipitation fraction that is lost by evaporation.

Key words: ecohydrology; keeling plots; transpiration; evaporation; gross ecosystem production; ecosystem respiration; water-use efficiency; mesquite; prosopis; understory.

Introduction

Natural and anthropogenic changes in the climate system will have large impacts on ecosystem structure and function. Within this context, there is a compelling need to understand how precipitation influences sources and sinks of CO_2 in seasonally dry ecosystems because these ecosystems would likely be more sensitive to changes in precipitation than to other global changes (Weltzin and others 2003). Net ecosystem production (NEP) is the net amount of carbon accumulated by the imbalance between gross

Received 9 December 2006; accepted 10 July 2007; published online 8 August 2007.
*Corresponding author; e-mail: yepezglz@unm.edu

ecosystem production (GEP) and ecosystem respiration (R_{eco}). Thus, the relationship between rainfall and carbon gain is determined by the degree of coupling between and the relative magnitudes of, GEP and R_{eco} when water is available. R_{eco} includes respiration from plants and microbes and as such is partially related to GEP. However, in seasonally dry environments, GEP and R_{eco} are often uncoupled due to distinct sensitivities of plant and soil microbial communities to infrequent moisture inputs (Huxman and others 2004). Overall, the degree of coupling between photosynthetic and respiratory activity in these seasonally dry ecosystems varies depending on the timing and duration of wetting and drying cycles and shows a marked contrast to systems that experience a more gradual change in water availability throughout a season (Jenerette and Lal 2005; Jarvis and others 2007).

In temperate ecosystems with no obvious dry season, ecosystem respiration is largely controlled by seasonal temperature fluctuations (Velentini and others 2000), such that early in the growing season the system rapidly starts accumulating carbon as photosynthesis up-regulates and canopy elements develop, whereas later in the season R_{eco} becomes an important flux (for example, Flanagan and others 2002; Huxman and others 2003). In seasonally dry ecosystems, this pattern is reversed because soon after the wet season starts, large quantities of CO_2 are lost to the atmosphere due to a rapid respiratory response of microbial communities to moisture availability, whereas a considerable photosynthetic flux may lag several days (Huxman and others 2004; Hastings and others 2005; Scott and others 2006a). The large increase of ecosystem respiration following rainfall (particularly after precipitation events occurring at the end of dry periods) has important consequences for the seasonal and annual net carbon balance (Saleska and others 2003; Lee and others 2004; Xu and others 2004; Huxman and others 2004; Hastings and others 2005; Scott and others 2006a, b; Jarvis and others 2007). However, factors controlling the magnitude and duration of this net ecosystem carbon loss are poorly understood, and consequences for the carbon sequestration potential of these ecosystems are unknown.

Following precipitation events, water can stimulate biological processes of plant and microorganisms after infiltrating in the soil or can be lost to the atmosphere after evaporating from the soil surface (Loik and others 2004). Unraveling the components of evapotranspiration (ET evaporation; E and plant transpiration T) is critical to understand how precipitation inputs impact carbon cycling in these ecosystems (Huxman and others 2005). GEP represents the photosynthetic activity of plants and therefore is fundamentally related to T due to the shared stomatal path of CO_2 and water exchange during photosynthesis. However, the relationships between R_{eco} to E and T are not well understood despite correlations between microbial and plant respiration and soil water availability. From an ecohydrological perspective, the influence of rain on NEP can be interpreted as the outcome of three related processes: the proportion of precipitation that is transpired by the plant community; the water-use efficiency of the vegetation (for example, photosynthetic CO_2 gain per unit of water transpired) and the precipitation fraction that is lost by evaporation (for example, without playing a role in photosynthetic gas exchange but potentially limiting plant and microbial activity by drying the surface) (Noy-Meir 1985). Based on this view, ecosystems with a higher transpiration to evapotranspiration ratio (T/ET) and higher water-use efficiency are expected to be more productive. However, the role of soil evaporation needs to be taken into account because this flux usually represents an important fraction of the available precipitation in semiarid environments (Huxman and others 2005; Lauenroth and Bradford 2006).

Transpiration in riparian mesquite woodlands along the upper San Pedro River in southeastern Arizona, USA is not very responsive to precipitation because trees have access to stable groundwater sources (Scott and others 2003). The phreatophytic nature of mesquite allows these ecosystems to be very productive by maintaining photosynthetic CO_2 gains during dry periods of the growing season (Scott and others 2004). However, the presence of a very conspicuous plant understory cover dominated by C4 perennial grasses and annual herbs during the peak rainy season in the late summer, and a large pool of labile soil organic matter and litter from mesquite for microbial decomposition produce highly dynamic patterns of NEP during the rainy season (Scott and others 2006b).

Stable isotopes of water have been recently used as a tool to partition the ET flux of entire ecosystems (Yepez and others 2003; Lai and others 2006), this technique relies on the fundamental differences in the isotopic composition between the fluxes contributing to ET (Yakir and Sternberg 2000). However, despite the potential of this tool for ecosystem studies, uncertainties related to the assumptions used to determine the isotopic composition of the contributing fluxes has hindered a wider application of these techniques. Careful examination of the assumptions involved in this method will greatly benefit the extended use of this powerful approach.

We investigated how the distribution of precipitation over a growing season influenced the dynamics of carbon and water cycling in semiarid riparian mesquite woodland. We took advantage of near-continuous measurements of NEP and ET, and the partitioning of their component fluxes using stable isotopes of water, to understand how water from growing season precipitation affects the ecosystem production. We specifically address three questions: (1) How does precipitation affect the coupling between GEP and R_{eco} in a seasonally dry mesquite woodland? (2) How are the components of ET related to the exchange of carbon dioxide in this system? (3) How do T/ET and vegetation water-use efficiency vary throughout the growing season?

Materials and Methods

Site Description

The study site was located within the San Pedro National Riparian Conservation Area in southeastern Arizona, USA (N 31°39′49′, W 110°10′39′; 1,191 m elevation). The climate in this region is semiarid with a bimodal distribution of precipitation. About 60% of the annual rainfall occurs as locally intense convective storms from July to September during the North American monsoon and about 23% occurs from December to March. The long-term average precipitation (1971–2000) at a nearby site is 358 mm (Tombstone AZ, Western Regional Climate Center). Soils were sandy loams. Vegetation at this upper floodplain terrace is mesquite (*Prosopis velutina* Wooton) woodland. The mesquite overstory does not form a closed canopy, and trees are not uniform in age or height. The overstory had an average height of 7 m, reaching a maximum height of approximately 10 m, with the lower main crown starting at approximately 5 m. In the understory, the perennial C4 grass sacaton (*Sporobulos wrightii* Munro ex Scribn) forms dense patches and annual herbs (mostly *Viguiera dentata* (Cav.) Spreng, *Lepidium thurberi* Wooton and *Chenopodium album* L.) are conspicuous during the peak rainy season in the late summer. Understory canopy cover was determined on 16th June, 14th August and 10th October of 2002 by visual assessment of either grasses or herbs in 80 1 m^2 quadrats placed in a stratified random fashion along eight 100 m transects. Leaf area index (LAI) of the tree canopy was measured with at LAI-2000 (Li-cor Inc., Lincoln NE, USA) on 16th June and 14th August along the same transects used for understory canopy cover.

Flux and Micrometeorological Measurements

The site was instrumented with a 14 m micrometeorological tower that continuously monitored general micrometeorological variables, ET and NEP with the eddy covariance technique. Details of the instrumentation, sampling protocol, accuracy of flux measurements and ET and NEP weekly means for the growing season of 2002 are given in Scott and others (2004). Daily ET measured at the tower was partitioned into ecosystem transpiration (T_e transpiration from trees and understory vegetation) and evaporation (E) based on the isotopic composition of water vapor on five days distributed over the growing season (see below). Evaporation estimates from these five days were then used to calculate a crop coefficient (K) after relating E with estimates of reference evaporation (ET_{ref}). Soil water content (θ_v) was measured with eight time domain reflectometers installed in profiles at depths of 0.05, 0.10, 0.20 and 0.30 m. Two probes were installed at each depth and the reported data for these depths represent an average of the two. Additionally, three probes were installed vertically to determine an average soil moisture over the top 0–0.30 m of the soil.

Mean weekly GEP was calculated from the mean weekly NEP and nighttime CO_2 exchange for 2002 (Scott and others 2004) by simply subtracting the mean weekly nighttime CO_2 rate from NEP. This approach assumes that nighttime respiration is representative of R_{eco} during the daylight hours despite the differences in temperature. We calculated the vegetation water-use efficiency (WUE) as the ratio of the mean weekly GEP over the mean weekly T_e. We used mean weekly averages to maintain consistency with results presented in Scott and others (2004). In this paper, positive values of NEP and its components indicate net gains to the ecosystem from the atmosphere.

ET Partitioning

We measured the isotopic composition of the different ecosystem water pools that contribute to ET and modeled the isotopic composition of the corresponding fluxes. Based on the isotopic composition of these components the ratio of transpiration to evapotranspiration (T/ET) was calculated from (Yakir and Sternberg 2000)

$$T/\mathrm{ET} = \frac{\delta_{\mathrm{ET}} - \delta_{\mathrm{E}}}{\delta_{\mathrm{T}} - \delta_{\mathrm{E}}} \qquad (1)$$

where δ_T is the isotopic composition of the transpiration vapor, δ_E is the isotopic composition of vapor

Table 1. Regression Parameters for Daytime Keeling Plots of Water Vapor

Period	n	r^2	Slope	y-intercept (δ_{ET})
D167				
Morning	14	0.43	−62.6 (20.7)**	−8.8 (2.4)
D226				
Morning	16	0.46	−38.4 (11.1)**	−10.0 (1.0)
Afternoon	15	0.14	−36.8 (25.1)	−9.1 (3.2)
Understory	15	0.14	44.0 (9.3)**	−13.5 (0.3)
D244				
Morning	16	0.78	−36.8 (25.1)**	−14.1 (3.2)
Afternoon	16	0.20	34.7 (18.3)*	−13.6 (3.2)
D257				
Morning	16	0.86	63.9 (6.6)**	−20.7 (0.8)
Afternoon	16	0.54	−30.3 (7.4)**	−13.9 (0.8)
D282				
Morning	16	0.78	−48.5 (6.7)**	−8.1 (1.2)
Afternoon	16	0.31	−28.5 (11.3)**	−10.3 (2.8)

*Numbers in parentheses are standard errors of the mean. Statistical significance at * α = 0.1 and ** α = 0.05.*

from soil evaporation and δ_{ET} is the isotopic composition of the ET flux. To determine δ_{ET} we produced Keeling plots (Yakir and Stenberg 2000) by regressing the isotopic composition of several vapor samples collected at five heights (0.1, 3, 7, 10 and 14 m) within the canopy profile against the inverse of the corresponding absolute humidity (Table 1). We partition ET on five dates during the growing season of 2002 representing environmental conditions characteristic of pre-monsoon (16th June, D167), monsoon (14th August, 1st September and 14th, D226, D244 and D257, respectively) and post-monsoon (9th October, D282) periods. Each day, vapor was collected during eight 30-min intervals. Four collection periods occurred between 8:00 and 12:00 h in the morning and four more in the afternoon between 14:00 and 18:00 h. Data were combined to produce two regressions representative of morning and afternoon periods. To assess the contribution to ET from understory transpiration during the peak-monsoon period (D226), we additionally collected vapor at four heights (0.5,1,1.5 and 2 m), four times a day, from a 2-m tall eddy covariance tower that measured ET below the tree canopy (see also Scott and others 2003).

Vapor was collected from air drawn from each height which continuously flowed through a set of five cryogenic (−80°C) glass traps at 0.3 l min^{-1}. Ten paired solenoid valves were sequentially programmed to open and close every 90 s to divert the flow to an infrared gas analyzer (Li-7000, LI-COR, Inc., NE, USA) prior to entering the traps and return the flow to the glass trap after vapor concentrations were recorded. The sequence was repeated every 7.5 min such that the vapor concentration from each height was measured four times over the 30 min collection period (Yepez and others 2003). Air flowing from the bottom height (0.1 m) was routed from three separate patches representing different ground covers; bare exposed soil, understory-grass litter cover and mesquite litter cover. Each air entry from the bottom heights was instrumented with a relative humidity sensor (Honeywell Sensing Products, El Paso, TX, USA) housed in a radiation shield while a copper-constantan thermocouple recorded soil temperatures just beneath the relative humidity sensor at approximately 0.05 m depth.

The isotopic composition of the soil evaporation flux (δ_E) was calculated from a modified form of Craig and Gordon (1965), which relates the relative humidity and the temperature of the evaporating surface to the fractionation processes that occur during evaporation. The expression for the overall fractionation in delta notation is provided in Yakir and Stenberg (2000):

$$\delta_E = \frac{\alpha^* \cdot \delta_{Surface} - h \cdot \delta_{atm} - \varepsilon_{eq} - (1-h) \cdot \varepsilon_k}{(1-h) + (1-h) \cdot \varepsilon_k / 1000} \quad (2)$$

where $\delta_{surface}$ is the isotopic composition of liquid water at the evaporating surface, and δ_{atm} is the isotopic composition of the background atmospheric water vapor. α^* is the temperature-dependent equilibrium fractionation factor (Majoube 1971). $\varepsilon_{eq} = (1 - \alpha^*) \times 10^3$. ε_k is the kinetic fractionation factor for oxygen (32‰; Cappa and others 2003) and h is the relative humidity normalized to

the temperature of the evaporating surface. To calculate δ_E with this model we used the average soil temperature and relative humidity recorded with the three ground probes, the isotopic composition of vapor collected at 0.1 m and the average isotopic composition of water from six to eight soil samples collected from the surface (top 0.2 m) near the ground sensors.

The isotopic composition of stem water and that of the transpiration flux is the same when transpiration occurs at isotopic steady state (ISS), however, this condition rarely occurs during diurnal transpiration cycles due to the transient changes of atmospheric conditions (Yakir and Sternberg 2000). We calculated the isotopic composition of transpired water from mesquite leaves under non-isotopic steady state conditions (δ_{TmNISS}) by first modeling values of transient leaf water enrichment between 6:00 and 18:00 h (Dogman and others 1974; Lai and others 2006) as:

$$\delta_{en}(t) = \delta_{es}(t) - [\delta_{es}(t) - \delta_{en}(t-1)] \exp\left(\frac{-\Delta t}{\tau\varsigma}\right) \quad (3)$$

where $\delta_{en}(t)$ and $\delta_{en}(t-1)$ are the non-steady state isotope composition of leaf water at predicted time t and at time $t-1$, respectively. Δt was a time interval of 900 s. $\delta_{es}(t)$ is the steady state oxygen isotope composition of water at the sites of evaporation in the leaf at time t. $\tau = W/T_{leaf}$; the turn over time of water in the leaf; where W is the molar concentration of leaf water and T_{leaf} is the leaf transpiration rate (mmol m^{-2} s^{-1}) of mesquite leaves. The ς term relates $\alpha^*\alpha_k(1-h)$, where α_k is the kinetic fraction factor (1.032; Cappa and others 2003), α^* and h are as in equation (2) but h was normalized to the infrared canopy temperature. T_{leaf} was measured on D226 in 4–5 mesquite leaves during different times of the day with a Ciras-1 photosynthesis system (PP systems, Hitchin, UK). To approximate T_{leaf} during the days lacking measurements we used the relationship between stomatal conductance (g_s) and vapor pressure deficit (D) obtained from chamber measurements on D226 and use D values measured at the tower during the corresponding days to predict g_s and T_{leaf}, we used a value of 6.1 mol m^{-2} as a fixed value for W in all our modeling efforts, this value produced a τ of about 3,000 s when estimated with measured values of T_{leaf} during the peak transpiration periods at around noon on D226. W was calculated as the difference in wet and dry weights per unit of leaf area of several leaflets collected at midday on D226. $\delta_{es}(t)$ was calculated following Yakir and Sternberg (2000) as:

$$\delta_{es}(t) = \delta_{stem} + (\delta_{ss} - \delta_{stem}) \cdot (1 - \exp^{-\rho})/\rho \quad (4)$$

where δ_{stem} is the isotopic composition of the stem water and δ_{ss} is the isotopic composition of bulk leaf water at isotopic steady state (ISS)

$$\delta_{ss} = \delta_{stem} + \varepsilon_{eq} + \varepsilon_k + h \cdot (\delta_{atm} - \varepsilon_k - \delta_{stem}) \quad (5)$$

where symbols are as above but δ_{atm} in this equation was from vapor collected at the 7 m height. The term ρ in equation (4) is a Peclet number that equals $(T_{leaf} \cdot L)/(C \cdot D_w)$ (Yakir and Stenberg 2000), C represents the molar concentration of water, D_w is the molar diffusivity of $H_2{}^{18}O$ in water, L is the effective mixing length in the leaf, here assumed to be 0.008 mm (Flanagan and others 1994). The isotopic composition of the transpiration flux from mesquite leaves under non-isotopic steady state (NISS) conditions (δ_{TmNISS}) was then calculated using the isotopic composition of non-steady state leaf water ($\delta_{en}(t)$) as the evaporating surface ($\delta_{surface}$) in equation (3) and using infra-red canopy temperatures for the computations of α^* and normalizing h to leaf temperature. We used the relative humidity and δ_{atm} measured at 7 m for these computations. This approach to model δ_{TmNISS} did not account for the small fractionation effects that occur at the boundary layer of the leaf surface (Flanagan and others 1991).

On D226 we compared modeled outputs of $\delta_{es}(t)$ and $\delta_{en}(t)$ with measured isotope ratios of bulk leaf water extracted from mesquite leaves five times during the day. We collected leaflets (removed from rachis) from sun-exposed branches of three different trees. Leaves were collected at times roughly corresponding to vapor collections (8:00, 10:00, 14:00, 16:00 and 18:00 h) on D226.

We collected suberized twig samples from six to eight different mesquite trees for isotope analysis of xylem water during each sampling period. The $\delta^{18}O$ of water from mesquite stems was used for δ_{stem} in equations (4) and (5). We also collected small portions of non-green shoots from below transpiring blades from six different grasses and six herbs growing close to the tower. The mean isotopic composition of water from stems of understory grasses and herbs was used as a proxy for the isotopic composition of understory transpiration (for example, assuming transpiration at ISS). We calculated the isotopic composition of ecosystem transpiration (δ_{Te}) computing the weighted average of δ_{Tm} and δ_{Tu} assuming $\delta_{Te} = 0.8\ \delta_{TmNISS} + 0.2\ \delta_{Tu}$. We used δ_{Te} values as δ_T in equation (1) to partition ET. Due to the relatively similar isotopic compositions of tree and understory xylem water, the weighting factors did not alter the calculation of T/ET in this ecosystem

(see also Yepez and others 2003). We compared estimates of T/ET assuming mesquite transpiration at ISS with T/ET estimates that took into account deviations of transpiration at ISS. When ISS transpiration was assumed $\delta_{stem} = \delta_{Tm}$ but to account for the deviation from ISS we used outputs of equations (2) and (3) to calculate δ_{TmNISS}.

To calculate daily E during the five days of isotope collection (referred as $E_{isotope}$) we multiply the mean value of morning and afternoon periods of estimates of T/ET during each day (assuming T/ET = 1 in the morning of D167, D226 and D282) by the ET flux measured with the eddy covariance system. This allowed us to estimate the evaporation component of ET in mm day^{-1}.

Soil, stem and leaves were collected in screw-capped borosilicate glass vials wrapped in Parafilm and transported to the lab in insulated containers. Water was extracted by cryogenic vacuum distillation (West and others 2006). Stable isotope ratio analyses were performed on a continuous flow isotope ratio mass spectrometer (Delta Plus, Thermo-Finnigan, San Jose, CA, USA) as in Yepez and others (2003). Our precision for repeated analysis of working standards was 0.2‰ for $\delta^{18}O$. δ values are in per mil (‰) on the V-SMOW scale.

Seasonal Evaporation

We constructed a simple evaporation model that allowed us to extrapolate estimates of T/ET from isotope and eddy covariance data though the growing season (here defined to be from DOY 121 to DOY 303). The model was based on estimates of reference evaporation (ET_{ref}; Shuttleworth 1993) and estimates of $E_{isotope}$ from the isotope-eddy covariance approach. We first calculated daily crop coefficients (K) during the 5 days when stable isotope measurements were available as:

$$K = \frac{E_{isotope}}{ET_{ref}} \tag{6}$$

where ET_{ref} (in mm) was determined by:

$$ET_{ref} = \frac{\Delta}{\Delta + \gamma*} \cdot (R_{net} - G) + \frac{\gamma}{\Delta + \gamma*} \cdot \frac{900}{T_{air}} \cdot U_2 \cdot D \tag{7}$$

where Δ is the gradient of the saturated vapor pressure curve at air temperature (kPa °C^{-1}),γ is the psychrometic constant (kPa °C^{-1}), γ* is the wind modified psychrometic constant (kPa °C^{-1}), R_{net} is net radiation (mm day^{-1}), G is soil heat flux (mm day^{-1}), T_{air} is the temperature of the air (°C), U_2 is the wind speed normalized to 2 m (m s^{-1}) and D is the vapor pressure deficit of the air (kPa). Meteorological variables measured at the tower were used to compute ET_{ref} with this equation. We then generated a polynomial equation that related K to the relative water content of the soil (RWC = θ_v/0.453) based on θ_v recorded at 0.05 m of the soil and assuming saturation at a θ_v of 0.453 m^3 m^{-3} (RWC; Ellsworth unpublished). With this equation we predicted daily K values (K_{model}) based on the daily estimates of RWC at 0.05 m depth. Modeled daily evaporation rates in mm (E_{model}) where then extrapolated through the growing season by:

$$E_{model} = K_{model} \cdot ET_{ref} \tag{8}$$

To compare estimates of E_{model} with independent assessments of evaporation, we calculated the upper and lower limits of daily seasonal evaporation by determining the daily loss of soil moisture (in mm) measured by the soil moisture probes. For days that did not register rainfall, we estimated the decrease in soil moisture for the upper 0.05 m and upper 0.30 m of soil by multiplying the daily change in average soil moisture ($\Delta\theta_v$) from the 0.05 and 0–0.30 m soil probes by their effective depths. Decreases in soil moisture from the 0.05 m layer were considered lower limits of evaporation because moisture changes in this depth would not account for water evaporated from very close to the surface ($< \sim 0.02$ m depth). Decreases in soil moisture in the top 0.30 m were considered as an upper limit for evaporation because some of the decrease in storage would be a result of infiltration beyond 0.30 m.

To determine understory plant transpiration (T_{under}) throughout the season, we relied on the understory transpiration fraction from the isotope-eddy covariance partitioning from D226, observations from Yepez and others (2003) and ET_{ref}. The contribution from tree transpiration (T_{tree}) to total ET was calculated from measurements of ET and subtracting modeled values of E_{model} and T_{under} so that our seasonal partitioning was constrained by the eddy covariance estimates of ET. We denoted the sum of T_{tree} and T_{under} ecosystem transpiration (T_e).

Results

Environmental Conditions

During the summer-fall growing season (May–October) total precipitation was 253 mm and only 11 out of 37 rainy days registered precipitation exceeding 5 mm. Precipitation from rainy days with less than 5 mm amounted to 16% of the total

precipitation received during this period. Most of the precipitation occurred during July (134 mm) with 17 days recording rain during this month. The average LAI of mesquite trees was 1.34 ± 0.14 m^2 m^{-2} on D167 and 1.45 ± 0.12 m^2 m^{-2} on D226. In the understory the ground cover was comprised of about 95% litter and 5% bare ground whereas the understory plant cover reached its maximum value in mid-August (Figure 1).

Total ET fluxes and environmental conditions of the studied season are reported in Scott and others (2004). During the five dates on which isotopic measurements were conducted, ET rates followed a typical diurnal trend reaching their maximum and staying constant for a few hours at midday (Figure 2) reflecting the progression of R_{net}, which peaked at approximately 1,000 Wm^{-2} around noon. Vapor pressure deficit (D) was below 3 kPa during the morning collection periods, and then rapidly increased between 8:00 and 12:00 h, except for D167 when D reached 3 kPa before 10:00 h. D was relatively constant early in the afternoon (between 3 and 4 kPa), but started declining around 16:00 h. Maximum T_{air} (32–36°C) lagged the peak in R_{net} by about 2 h. Mean θ_v at the top 0.25 m varied substantially among collection days ranging from 0.01 m^3 m^{-3} before the monsoon (D167) to 0.05 on D226, 0.07 on D244, 0.09 on D257 and 0.05 on D282.

ET Partitioning

Modeled values of leaf water enrichment $\delta_{en}(t)$ showed the same diurnal trend as measured values of bulk leaf water on D226 (Figure 3B) and both were consistently below the expected values under isotopic steady state (δ_{es}(t)). Measured vales were consistently lower than ($\delta_{es}(t)$) and $\delta_{en}(t)$ during the morning by 3 and 2‰, respectively. During the afternoon measured and modeled values converged. Differences between $\delta_{es}(t)$ and $\delta_{en}(t)$ are within the range expected for leaves with short water turnover times (Lai and others 2006) as is the case of mesquite leaves, however differences between $\delta_{en}(t)$ and measured enrichments are probably due to the expected differences between isotopic composition of bulk leaf water and the water at the sites of evaporation (for example, due to ρ in equation 4; Yakir and Sternberg 2000) or for not representing the turnover time of leaf water appropriately in our computations (for example, use of a fixed value; Lai and others 2006). Consistency on the modeled diurnal trends of $\delta_{en}(t)$ allowed us to predict the δ_{TmNISS}. Modeled $\delta^{18}O$ values of transpiration from mesquite leaves indicated that trees did not transpire at ISS during most of the day (Figure 3A). In all cases the deviation from ISS was more pronounced between 8:00 and 10:00 h and was at minimum between 14:00 and 16:00 h. To include the effect of these deviations in our computations of T/ET (equation 1) we used the average ‰ deviation during the periods of vapor collection (Figure 2) to compute the expected values of δ_{TmNISS} during these periods of the day (Table 2).

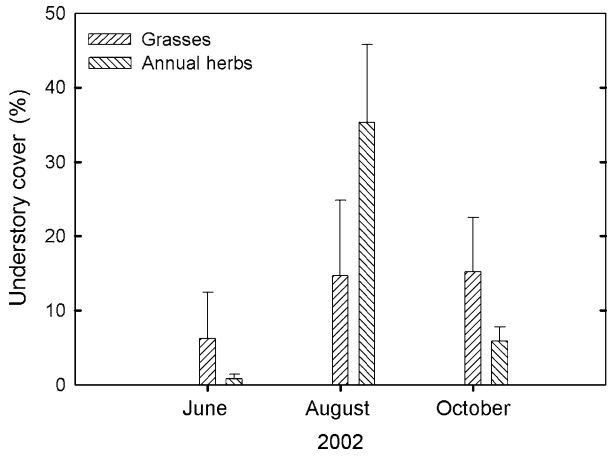

Figure 1. Canopy cover of understory vegetation during the summer of 2002 at the mesquite woodland. *Error bars* represent standard deviations from measurements in 80 1 m^2 quadrants.

The modeled isotopic composition of vapor from soil evaporation (δ_E) was strongly depleted in heavy isotopes and varied considerably through time, with the estimated values showing a strong dependence on the original isotopic composition of soil water (δ_{soil}; Table 2). We do not have information on the potential gradients of isotopic composition in water within the 0.02 m soil layer which could affect the value of $\delta_{surface}$ used in the calculations of δ_E. Soil water potential (ψ_{soil}) can be predicted from: ψ_{soil} (MPa) = 0.00006 $\theta_v^{-3.46}$ in our site (P. Ellsworth, personal communication), therefore suggesting that the evaporation front could occur when θ_v is above 0.04 m^3 m^{-3} (Konukcu and others 2004). This condition was not met on D167 when the top 0.02 m of the surface was too dry and the evaporation front probably occurred below 0.02 m. Estimates of δ_E on this date should be seen with caution. However, during the rest of the sampling days, ψ_{soil} in the top 0.02 m of the soil was above (more positive) a critical ψ_{soil} (−7 MPa) to permit liquid diffusion in a sandy soil and thus allow an evaporation front in this region (Konukcu and others 2004).

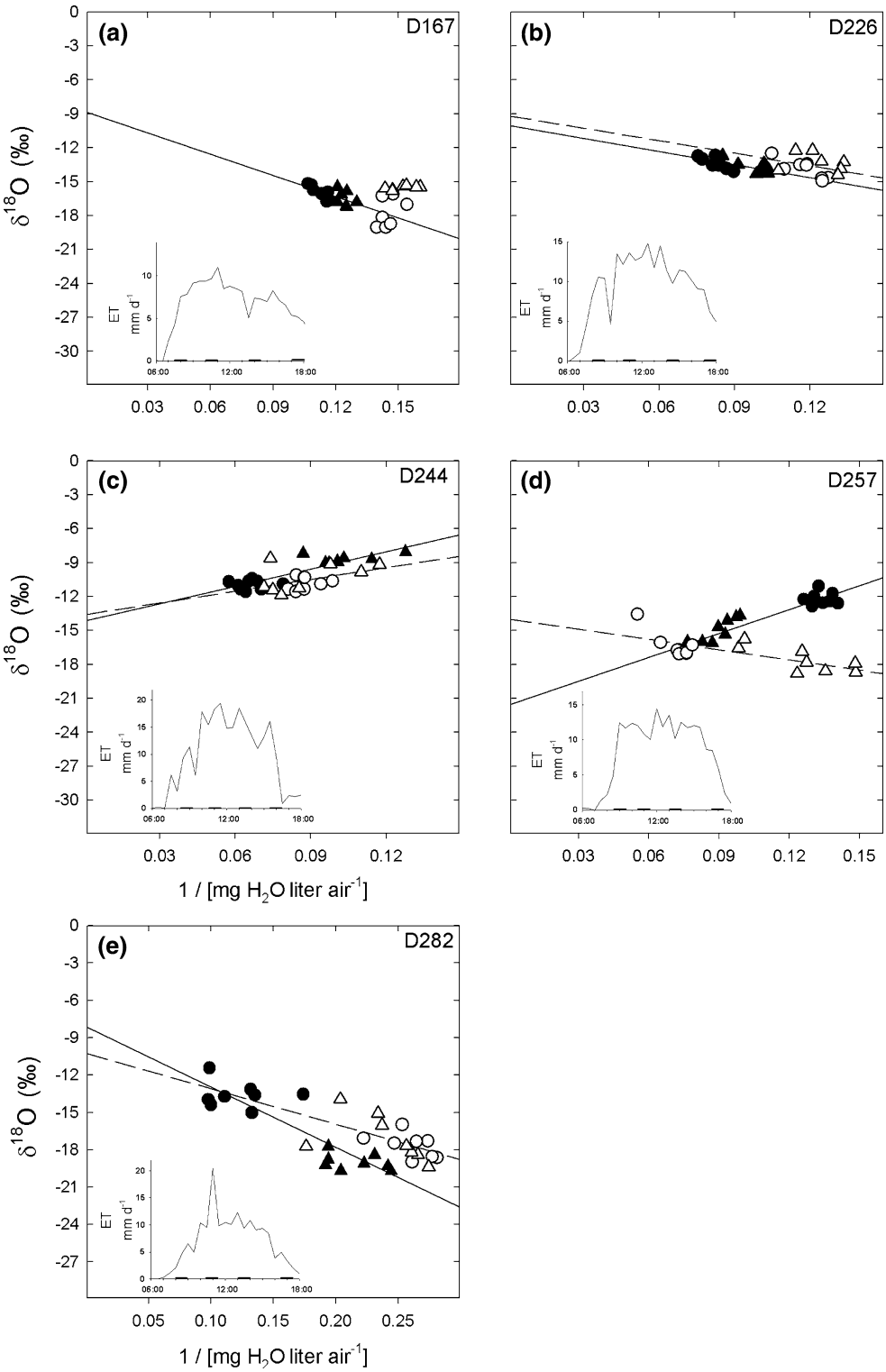

Figure 2. Daytime Keeling plots of water vapor produced on five dates during the growing season of 2002 in a semiarid mesquite woodland. The *y*-intercept indicates the isotopic composition of the ET flux (δ_{ET}). *Different symbols* indicate collection periods throughout a single collection day. *Dark symbols* represent collection periods in the morning and *open symbols* indicate collection periods in the afternoon. Regression parameters are given in Table 1. *Insets* are diurnal ET trends for the corresponding days measured with the eddy covariance technique (Scott and others 2004); marks on the *x*-axis indicate the periods on which vapor was collected.

Keeling plots of water vapor indicated that *T*/ET was not constant through the growing season (Figure 2; Table 1). During dry periods (D167, D226 and D282) δ_{ET} was more similar to the isotopic composition of transpiration, whereas δ_{ET} deviated from isotopic composition of transpiration on D244 and D257 when the soil surface was wet (Table 2). During D226 total ET was 4.9 mm day^{-1} and understory ET was 1.7 mm day^{-1}. Based on these values, we estimated that understory transpiration was 1.2 mm day^{-1} or 25% of total ET on this day (for example, 0.71 × 1.7 mm day^{-1}).

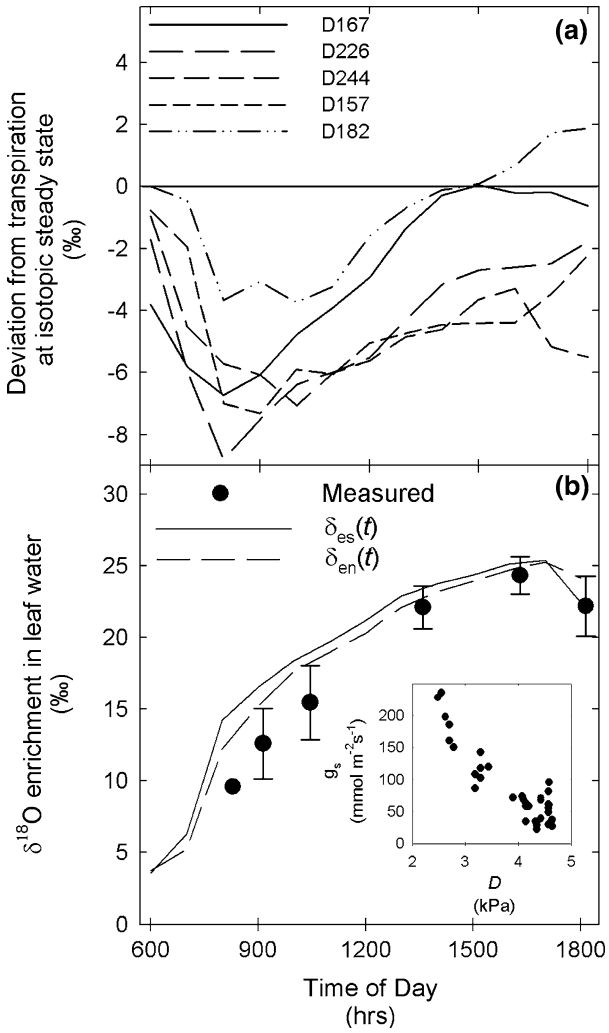

Figure 3. Diurnal trend of deviation from isotopic steady state (*dashed line*) in predicted $\delta^{18}O$ values of water vapor from transpiring mesquite leaves during five different days (**A**). Modeled and measured values of isotopic leaf water enrichment in mesquite trees on D226 (**B**), δ_{es} is the predicted enrichment at isotopic steady state, δ_{en} (t) is the leaf enrichment under non-isotopic steady state conditions and *black symbols* indicate measured isotopic ratios of bulk leaf water from leaves collected at different times of the day. Values are means (n = 3) plus or minus one standard error. *Inset* shows the relationship between stomatal conductance (g_s) and vapor pressure deficit (D) on D226.

Seasonal Trend of ET and NEP Components

Results from the evaporation model allowed us to extrapolate the evaporation trends calculated from isotope measurements throughout the growing season and therefore account for the components of ET measured with the eddy covariance tower. The empirical equation to estimate K_{model} is displayed in Figure 4A. This equation allowed us to estimate values of E_{model} that were between the upper and lower limits of evaporation suggested by changes in soil moisture at different depths (Figure 4B). Notably, E_{model} values were closer to the lower limits of evaporation during dryer periods and approached the upper limits when evaporation rates where the highest (Figure 4B).

During the peak growing season period (D226), understory transpiration was 18 ± 0.4% of ET_{ref} whereas late in the growing season of 2001 (Day 265; Yepez and others 2003) this fraction was 11 ± 2%. Based on the average of these periods we assumed that understory transpiration (T_{under}) was 15% of ET_{ref} from the start of the rainy period (DOY 187) to DOY 282 when understory canopies were largely senescent (Figure 1).

Cumulative evaporation during the whole season (78 mm) represented 31% of the precipitation (253 mm; Table 3). Tree transpiration was the principal component of ET throughout the growing season (Figure 5) amounting to 473 mm during the studied period. Furthermore, assuming that runoff and deep percolation were negligible, and that interception loss is included in our estimates of E, we can indirectly estimate that mesquite trees used about 97 mm of rainwater by subtracting the sum of T_{under} and E (157 mm) from the total amount of precipitation received during the studied period (Table 3). Similarly, T_{tree} exceeded precipitation inputs by 87% (Table 3), suggesting that mesquite trees used 377 mm from ground and deep vadose zone water. Understory transpiration throughout the season constituted 31% of precipitation (Table 3). Overall, T_e amounted to 552 mm through the season which suggested a seasonal T/ET of 0.90 (Table 3). There was likely some interception loss that was not properly accounted for by our approach and this should be kept in mind when interpreting the results.

As mesquite trees started to leaf out in May, R_{eco} and GEP showed a strong coupling as both fluxes slowly increased until they leveled out and maintained constant values in June. The system was a net sink of CO_2 during June (Table 3). Interestingly, 2 weeks after the start of the rainy period (July) GEP gradually started increasing until it reached its maximum values in mid August. Following its peak, GEP gradually declined until October when GEP had decreased to pre-monsoon levels (Figure 5). Notably, maximum GEP occurred during the period when understory cover was also at maximum (Figure 1). Nighttime R_{eco} was more responsive than GEP to precipitation during the

Table 2. Isotopic Composition of Ecosystem Water Sources Contributing to ET and the Ratio of Transpiration to Evapotranspiration (*T*/ET)

Assuming ISS							Assuming deviation from ISS			
Sampling period	δ_{soil} (0.2 m)	δ_E	$\delta_{Tm\text{-}ISS}$	δ_{Tu}	$\delta_{Te\text{-}ISS}$	*T*/ET	Mean deviation from ISS	δ_{TmNISS}	δ_{Te}	*T*/ET
DOY 167										
(700–1100 h)	2.9 (1.1)	−33.1 (2.0)	−7.7 (0.4)	−0.7(0.04)	−6.3 (0.4)	0.91 (0.09)	−5.6 (0.9)	−13.3 (0.9)	−10.8 (0.7)	1.09 (0.10)
DOY 226										
(800–1130 h)	1.5 (3.2)	−35.4 (5.5)	−6.5 (0.5)	−4.6 (0.9)	−6.0 (0.5)	0.86 (0.04)	−6.6 (0.2)	−13.1 (0.9)	−11.4 (0.3)	1.08 (0.04)
(1400–1600 h)	1.5 (3.2)	−36.2 (3.7)	−6.5 (0.5)	−4.6 (0.9)	−6.0 (0.5)	0.90 (0.10)	−2.3 (1.3)	−8.8 (1.2)	−8.0 (1.2)	0.96 (0.11)
Understory	1.5 (3.2)	−35.8 (4.6)		−4.6 (0.9)		0.71 (0.02)				
DOY 244										
(830–1130 h)	5.8 (2.8)	−31.6 (4.7)	−6.5 (0.3)	−2.5 (1.2)	−5.3 (0.9)	0.66 (0.12)	−6.4(0.6)	−12.9 (0.6)	−10.8 (0.7)	0.84 (0.15)
(1300–1630)	5.8 (2.8)	−31.1 (3.7)	−6.5 (0.3)	−2.5 (1.2)	−5.3 (0.9)	0.63 (0.14)	−4.0 (1.0)	−10.5 (1.0)	−8.8 (1.0)	0.76 (0.14)
DOY 257										
(830–1130 h)	−1.5 (1.4)	−41.0 (2.7)	−5.4 (0.6)	−3.2 (0.9)	−4.7 (0.7)	0.56 (0.02)	−6.6 (0.8)	−11.9 (0.8)	−10.2 (0.8)	0.65 (0.03)
(1400–1730 h)	−1.5 (1.4)	−40.0 (1.6)	−5.4 (0.6)	−3.2 (0.9)	−4.7 (0.7)	0.74 (0.02)	−4.3 (0.4)	−9.7(0.4)	−8.4 (0.5)	0.82 (0.03)
DOY 282										
(800–1130 h)	−3.1 (2.1)	−42.0(5.5)	−7.8 (0.4)	−4.4 (0.6)	−7.2 (0.4)	0.97 (0.04)	−3.2 (1.2)	−10.9 (1.2)	−9.6 (1.1)	1.04 (0.04)
(1400–1730 h)	−3.1 (2.1)	−41.4 (2.3)	−7.8 (0.4)	−4.4 (0.6)	−7.2 (0.4)	0.91 (0.08)	0.5 (0.7)	−7.0 (0.7)	−6.5 (0.7)	0.89 (0.08)

δ_E is the modeled isotopic composition of evaporation. δ_{Tm}, δ_{Tu} and δ_{Te} are the isotopic compositions of transpiration from mesquite trees, from understory vegetation and ecosystem transpiration, respectively, numbers in parentheses are the standard deviation (SD). δ_{soil} is the isotopic composition of soil water in the top 0.2 m of the soil with values in parenthesis expressing the SD of six to eight samples. T/ET was calculated with equation (1) considering δ_{Te} as an expression of δ_T and either assuming transpiration at isotopic steady state (ISS) or assuming mesquite transpiration deviating from ISS. Error propagation in estimates of T/ET was determined using isoerror V4 (Phillips and Gregg 2001) considering the SD in δ_E, the SD in δ_{Te} and the standard errors of the Keeling-plot intercepts.

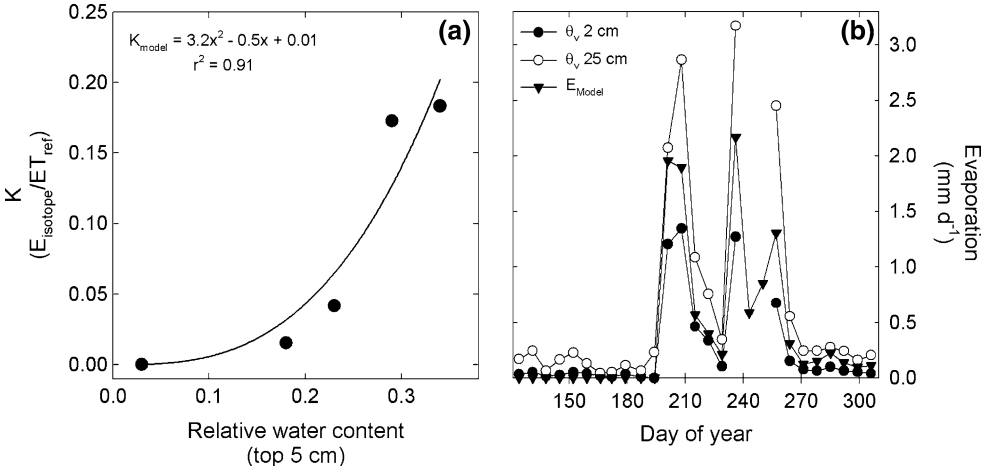

Figure 4. Relationship between the measured crop factor (K) and the relative soil water content (RWC) on the five days when isotope measurements were available (**A**). Predicted values of evaporation (E_{model}; *inverted triangle*) in relation to upper and lower limits of evaporation based on changes on soil water content at two different soil depths.

rainy period. R_{eco} showed an immediate increase following moisture inputs into the shallow soil layers (Figure 5). In fact, during the wettest part of the season (July–August), R_{eco} was extremely high and the system became a net source of CO_2 to the atmosphere. During July (the wettest month of the season) the system lost an equivalent of 46% of the net carbon accumulation observed during the whole growing season (Table 3). After the peak of the monsoon, R_{eco} started to decreased and tracked GEP despite continued precipitation in August and September. Despite the large respiratory fluxes observed during the rainy period, the system was a net carbon sink during the growing season of 2002. From May to October the ecosystem accumulated 114 g C m^{-2} (Table 3). Weekly GEP and T_e were positively correlated through the growing season, but the slope of this relationship differed between dry and wet periods (Figure 6). Through the season, transpiration rarely exceeded 5 mmol H_2O m^{-2} s^{-1}. Weekly values of vegetation water-use efficiency were negatively correlated to weekly D means (Figure 6). Notably, the system registered its lowest WUE values before the rainy season and showed the highest WUE values soon after the wettest period in July when the understory vegetation was developing.

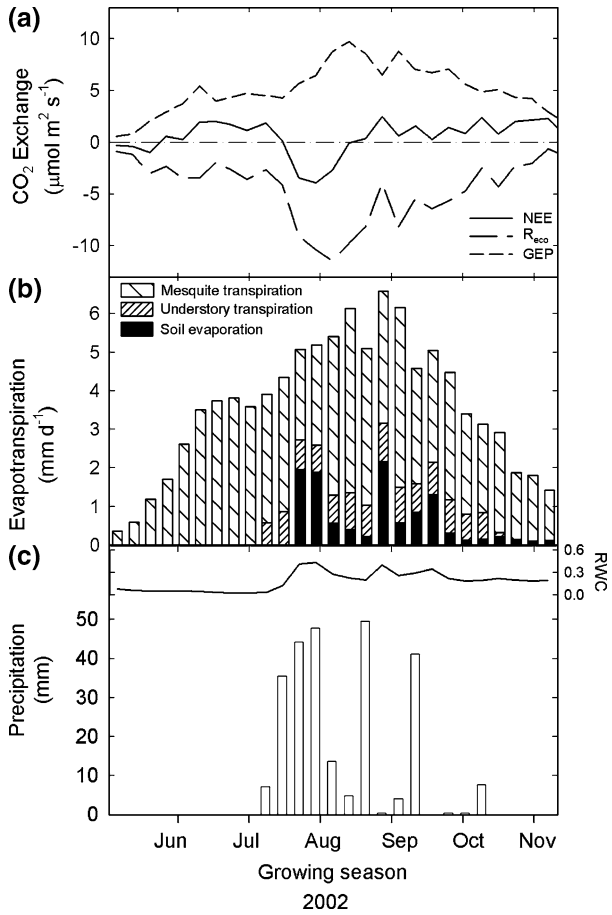

Figure 5. Seasonal pattern of weekly averaged ecosystem carbon dioxide exchange (**A**), evapotranspiration components (**B**) and precipitation and relative water content (top 5 cm) of the semiarid mesquite woodland (**C**). ET flux components and T/ET were calculated based on the isotopic flux partitioning, soil evaporation modeling and measurements of ET with the eddy covariance technique.

Discussion

Factors Controlling GEP and R_{eco} During Wet and Dry Periods

Patterns of CO_2 exchange and evapotranspiration in the mesquite woodland were different during wet and dry periods of the growing season, and as the season progressed, the factors controlling the magnitude and variation of these fluxes appeared

Table 3. Monthly Totals for Carbon and Water Fluxes of a Semiarid Mesquite Woodland in Southeastern Arizona, USA for the Year 2002

	P mm	E mm	T_{under} mm	T_{tree} mm	T_e mm	ET mm	T/ET	R_{eco} g C m^{-2}	NEP g C m^{-2}	GEP g C m^{-2}
May	0	0	0	42	42	42	1.00	−72	−5	67
June	0	0	1	108	109	109	1.00	−91	51	142
July	134	29	23	82	104	134	0.78	−235	−52	183
August	70	25	28	105	133	158	0.84	−254	16	271
September	42	18	23	75	98	116	0.84	−167	35	202
October	8	5	4	62	67	71	0.93	−81	68	148
Season totals	253	78	79	473	552	630	0.90	−900	114	1,014

P represents precipitation.

to be different. GEP and R_{eco} were well coupled during dry periods, but not towards the beginning of the rainy period when R_{eco} increased dramatically in response to first rain events of the monsoon period. However, the respiratory response to precipitation was dampened as the rainy season progressed. Overall, the woodland acquired increasing amounts of carbon through the growing season mainly due to declines in R_{eco} (Figure 5). Over the whole growing season, the ecosystem was a net carbon sink despite substantial CO_2 losses during the rainy period (Table 3).

During the dry period prior to monsoon rains, GEP and R_{eco} were tightly coupled, reflecting the metabolic activity of mesquite growth. For example, during May the system was a small source of CO_2 to the atmosphere likely as a result of increasing rates of growth respiration for leaf and root construction (Williams and others 2006, Figure 5). However, in June, when trees were fully leafed out, the system became a net CO_2 sink (Table 3). The control of ecosystem fluxes by mesquite trees during the dry period was supported by the pattern of T/ET and WUE (Figures 5, 6). During this pre-monsoon period, ET rates mirrored the gradual increase in GEP and T/ET approached 1.0 suggesting that mesquite transpiration was the sole contribution to ET. The understory vegetation was largely inactive and the soil surface very dry. Plant transpiration correlated well with GEP during these dry months (Figure 6) and therefore likely reflected the water-use efficiency of mesquite trees. WUE during this dry period was influenced by D (Figure 6).

The onset of precipitation triggered very dynamic periods of water and CO_2 exchange. During the wettest part of the season, GEP and R_{eco} in this riparian woodland were largely decoupled; the system experienced substantial losses of CO_2 to the atmosphere that were not proportional to the gradual increases in GEP (Figure 5). This rapid change from CO_2 sink to source had important consequences for NEP because CO_2 losses were sustained for several weeks. During one single month (July), the woodland lost an equivalent of 46% of the net carbon gain recorded during the 6-month study period (Table 3).

Large CO_2 losses following precipitation events are an important control on the carbon sequestration potential in seasonally dry ecosystems (Xu and others 2004; Huxman and others 2004). Mass displacement of CO_2 from soil pores when water infiltrates (Xu and others 2004), rapid up regulation of metabolic activity of soil microbial communities (Fierer and Schimel 2003; Austin and others 2004), the availability of labile organic matter for microbial decomposition (Jarvis and others 2007), duration of soil moisture at the soil surface (Xu and others 2004) and the increase of plant respiration for growth and maintenance as leaf area and roots develop (Flanagan and others 2002), all contribute to the large CO_2 efflux following moisture inputs. However, the relative importance of these processes on the degree of coupling of GEP and R_{eco}, (hence the duration and magnitude of carbon losses) vary through time, and each respond in different ways to changing environmental conditions.

The dynamics of CO_2 exchange during the rainy period in the mesquite woodland illustrate the trade-off among some of these mechanisms. Early during the rainy period, when large CO_2 effluxes were observed, GEP and R_{eco} were largely decoupled. Litter production in this ecosystem is in disequilibrium with current climate because of tree access to stable groundwater (Scott and others 2006b). As a consequence, the system accumulates large quantities of soil labile organic material because the period of higher litter production (fall or early winter) does not coincide with optimal

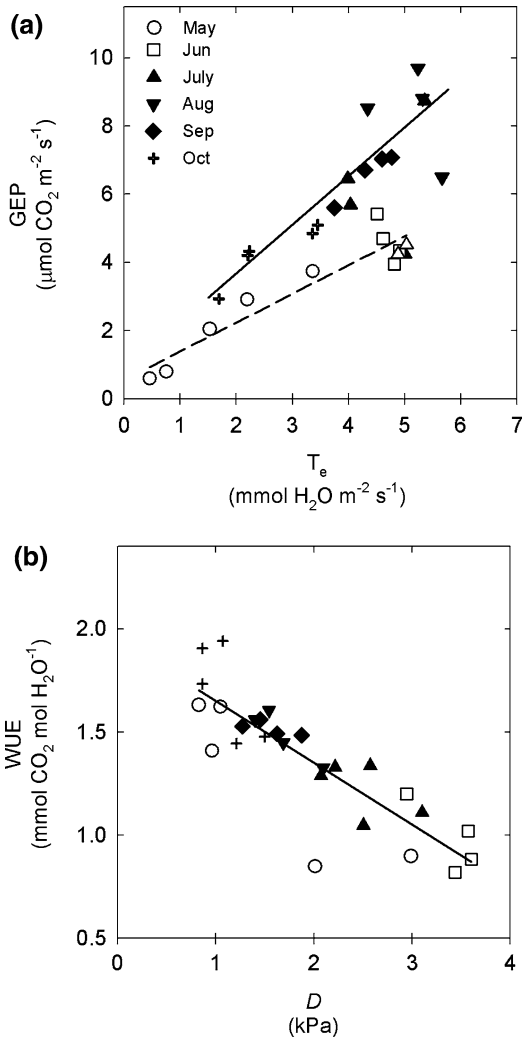

Figure 6. Relationship between (**A**) mean weekly ecosystem transpiration (T_e; trees and understory) and gross ecosystem production (GEP) and (**B**) mean weekly vegetation water-use efficiency (WUE = GEP/T_e) versus mean weekly vapor pressure deficit. Regression coefficients in (**A**) for the dry period were $y = 0.84x - 0.55$, $r^2 = 0.89$ and $y = 1.42x + 0.82$ r^2 0.91 for the wet period.

environmental conditions (moisture and temperature) necessary to support decomposition. The large CO_2 ecosystem losses observed early in the monsoon season likely resulted from the rapid decomposition of this large labile pool of organic material that induced a strong respiratory response from soil microbial communities as the soil surface was moistened by summer rains (Austin and others 2004; Williams and others 2006). This carry over effect on R_{eco} highlights the importance of dry periods on the subsequent response of seasonally dry ecosystems to rainfall (Saleska and others 2003; Jarvis and others 2007). An additional factor that likely contributed to the pronounced R_{eco} during this early rewetting period is the respiratory flux from tissue construction and maintenance as the understory vegetation rapidly developed following precipitation events (Williams and others 2006), although the relative contribution to R_{eco} from these processes remains uncertain. The response of R_{eco} to precipitation events later in the rainy period was less pronounced than early in the season and R_{eco} appeared to track GEP while the system became a net sink of CO_2 (Figure 5). The less pronounced response of R_{eco} to precipitation later in the season may in part be attributable to the change in the pool size of labile carbon for decomposition and nutrients at the soil surface layers. Substantial use of labile soil carbon and nutrients by microbes (Saetre and Stark 2005), gaseous losses (McLain and Martens 2006), modification of soil aggregates and microbial stress to wetting and drying cycles (Fierer and Schimel 2003) and active shallow rooted understory vegetation may have contributed to these reductions in pools sizes.

Relationship between ET Components and Carbon dioxide Exchange

Understanding the timing and magnitude of plant transpiration and evaporation as separate processes provides means to mechanistically link hydrological processes and ecosystem productivity (Noy-Meir 1985). Integrated over the growing season T/ET was 0.90 at our mesquite woodland, a value that is considerably higher than what is commonly observed in other dryland ecosystems (Huxman and others 2005; Scott and others 2006a). This high T/ET ratio reflects the ability of mesquite trees to access groundwater and reinforces the idea that plant activity is partially decoupled from precipitation events in this system (Scott and others 2003). However, precipitation did trigger very active periods of water and carbon exchange controlled by the duration of moisture at the soil surface. For example, the onset of precipitation stimulated the development of understory vegetation (Figure 1), whose transpiration accounted for about 31% of the total ET flux during the peak monsoon season (Table 3). Similar to other savanna-like ecosystems the understory vegetation strongly determined the availability of soil moisture and therefore directly influenced the temporal patterns of NEP (Hutley and others 2001).

Following the onset of rainfall, evaporation also increased and comprised an important fraction of ET and, therefore, influenced the duration of

moisture at the soil surface. During the 6-month study period, 31% of the available water from precipitation returned to the atmosphere through this pathway (Table 3). This large fraction of precipitation lost as evaporation suggests that the rain-use efficiency of this ecosystem is generally low because trees and understory vegetation only used 38 and 31% of the available precipitation, respectively. However, the sensitivity of R_{eco} to soil moisture and temperature (Jarvis and others 2007) suggests that E likely plays an important role in the dynamics of carbon cycling by cooling the soil surface and rapidly removing soil water that would otherwise by available for plant and microbial activity. For example, the dampened response of R_{eco} to precipitation inputs later in our study period may be partially explained by the ephemeral duration of shallow soil moisture as sustained rates of soil evaporation during August and September may have contributed to a rapid depletion of shallow soil moisture that was not recharged by continued precipitation events (Figure 5). Overall, the impact of E on productivity in seasonally dry ecosystems needs to be investigated in the context of the size and distribution of precipitation events throughout the growing season.

An additional factor playing a role in the net ecosystem production as a function of precipitation is the water-use efficiency of the vegetation. Vegetation water-use efficiency (WUE) is the ratio of photosynthetic CO_2 assimilation to the amount of water lost by transpiration. In seasonally dry ecosystems, this ratio reflects the ability of plants to adjust their photosynthetic capacity to the restrictions imposed by stomatal regulation to avoid desiccation (Fisher and Turner 1978). Therefore, variation in WUE as precipitation and associated resources become available may explain the sensitivity of GEP to diversity of plant functional type composition. Differences in water-use efficiency among plants possessing C3 and C4 metabolic pathways are well documented (Ehleringer and Monson 1993), with C4 plants generally displaying higher efficiencies in relation to C3 plants in semiarid ecosystems. In the woodland, despite the ability of mesquite trees to use groundwater and avoid desiccation, the vegetation WUE gradually increased as the season advanced (Figure 6). The understory vegetation was significantly composed of C4 grasses (Figure 1). Thus, the increase in WUE following the onset of rain may be partially attributed to the enhanced capacity of understory plants to assimilate CO_2. The lower daily vapor pressure deficits (D) that occurred after the onset of rain may have also contributed to the higher WUE (Figure 6). As the vapor pressure gradient between the leaves and the air increases (for example, in proportion to D), more water is lost through transpiration during photosynthesis and hence water-use efficiency is reduced (Nobel 1999). Therefore, if the access to stable groundwater sources allowed mesquite leaves to maintain a relatively constant stomatal conductance during the growing season, WUE would be higher at lower D. The ability to estimate an ecosystem-level WUE independent of the dynamics of soil evaporation facilitates the understanding of the metabolic control of plants to the net ecosystem fluxes as they respond to rainfall.

Assumptions Involved in the Isotopic ET Partitioning

The use of Keeling plots of water vapor to determine δ_{ET} assumes that only two sources contribute vapor to the ecosystem boundary layer (for example, the atmospheric background and the contributing ecosystem fluxes) and that the relative contribution of such sources remain constant thought time (Yakir and Sternberg 2000). We try to minimize the effects of changing environmental conditions and ET rates by sampling vapor during 30-min periods; a period of time on which the relative contributions of vapor sources were assumed to remain constant. Based on this strategy, we expected to calculate T/ET on each individual period to then provide an average estimate of the diurnal proportions of the fluxes contributing to ET. However, in many cases the isotope and moisture gradients needed to create a linear regression were absent (Figure 2). We, therefore, opted to generate regressions that explained morning and afternoon periods. With this approach we obtained reasonable regression coefficients in our Keeling plots (Table 1) and, overall, data from these periods showed the same trends suggesting that these may be points in time on which the relatively contributions of vapor to the canopy boundary layer by different components remained relative constant.

Dynamics of isotopic enrichment of leaf water are usually discrepant from modeled isotopic enrichments assuming ISS (for example, based on Craig and Gordon1965; Lai and Others 2006). These differences are in part due to the turnover time of leaf water and the typical diurnal variation of atmospheric moisture (Farquhar and Cernusak 2005). Consideration of deviations from ISS is relevant for ET partitioning studies because the transient enrichment of leaf water also affects isotopic composition of the transpiration flux (δ_T; Figure 3).

Estimates of the isotopic composition of transpiration based on the isotopic leaf water enrichment in mesquite leaves suggest that these trees did not transpire under ISS during most of the day. During the morning periods, deviation from ISS varied from about to 3 to 9‰ depending on the collection day whereas the deviation in the afternoon varied between 0 and 6‰. Failure to account for these deviations by assuming that transpiration occurred at ISS could carry an error of 6 to 22% in our final estimates of T/ET (Table 2). Overall, not accounting for the expected deviations from ISS on each collection day would have a dramatic impact in our final estimates of seasonal evaporation and therefore on the estimated contributions of understory, and tree transpiration to seasonal ET and the water-use efficiency of the vegetation. If transpiration of mesquite leaves would have been assumed at ISS we would have estimated seasonal values of E_{model} and T_{tree} of 104 and 456 mm, respectively with an overall ecosystem T/ET of 0.80; a 10% difference. Furthermore, if mesquite transpiration at ISS was assumed, the slope of the relationship between GEP and T_e would have indicated a gain of 1.06 μmol of CO_2 per mmol of water lost during the dry periods and 1.22 μmol of CO_2 per mmol of water lost during the wet period, a 19 and 16% change, respectively. Clearly, accounting for the potential deviation of transpiration from ISS is key to appropriately determine the end members of a mass balance approach to partition ET.

Advancing understanding about the functioning of seasonally dry ecosystems is fundamental to test predictions on how these ecosystems would respond to climate change. In semiarid woodlands, the consequences of anticipated changes in precipitation regimes towards larger precipitation events and longer drought periods (Weltzin and others 2003) demands particular attention due to the potential alteration of the carbon sink strength of these ecosystems via imbalances between photosynthesis and respiration following precipitation events after dry periods. A step towards this new synthesis can only be given if the components of the ecosystem water cycle are understood as separate processes influencing different functional and structural ecosystem properties.

ACKNOWLEDGMENTS

We were able to carry out this work thanks to financial support from the SAHRA-NSF Science and Technology Center (EAR-9876800), the Upper San Pedro Partnership and CONACYT-Mexico for granting a graduate fellowship (150496) to EAY. Patrick Ellsworth, Joost van Haren, Danielle Pierce, Rico Gazal and Marcela Lopez provided invaluable support and an anonymous reviewer provided comments to improve this manuscript.

REFERENCES

Austin AT, Yahdjian L, Stark JM, Belnap J, Porporato A, Norton U, Ravetta D, Schaeffer S. 2004. Water pulses and biogeochemical cycles in arid and semiarid ecosystems. Oecologia 141:221–35.

Cappa CD, Hendricks MB, DePaolo DJ, Cohen RC. 2003. Isotopic fractionation of water during evaporation. J Geophys Res 108:4525.

Craig H, Gordon LI. 1965. Deuterium and oxygen-18 variations in the ocean and the marine atmosphere. In: Tongiori E, Ed. Proceedings of the conference on stable isotopes in oceanographic studies and paleotemperatures. Pisa: Laboratory of Geology and Nuclear Science. pp 9–130.

Dongmann G, Nürnberg HW, Förstel H, Wagener K. 1974. On the enrichment of $H_2{}^{18}O$ in the leaves of transpiring plants. Rad Environ Biophys 11:41–52.

Ehleringer JR, Monson RK. 1993. Evolutionary and ecological aspects of photosynthetic pathway variation. Ann Rev Ecol Syst 24:411–439.

Farquhar GD, Cernusak LA. 2005. On the isotopic composition of the leaf water in the non-steady state. Funct Plant Biol 32:293–03.

Fierer N, Schimel J. 2003. A proposed mechanism for the pulse in carbon dioxide production commonly observed following the rapid rewetting of a dry soil. Soil Sci Soc Am J 67:798–05.

Fisher RA, Turner NC. 1978. Plant productivity in the arid and semiarid zones. Ann Rev Plant Physiol 29:277–317.

Flanagan LB, Comstock JP, Ehleringer JR. 1991. Comparison of modeled and observed environmental influences on the stable oxygen and hydrogen isotope composition of leaf water in *Phaseolus vulgaris* L. Plant Physiol 96:588–96.

Flanagan LB, Phillips SL, Ehleringer JR, Lloyd J, Farquhar GD. 1994. Effect of changes in leaf water oxygen isotopic composition on discrimination against $C^{18}O^{16}O$ during photosynthetic gas exchange. Aust J Plant Physiol 21:221–34.

Flanagan LB, Wever LA, Carrlson PJ. 2002. Seasonal and interannual variation in carbon dioxide exchange and carbon balance in a northern temperate grassland. Glob Change Biol 8:599–15.

Hastings SJ, Oechel WC, Muhlia-Melo A. 2005. Diurnal, seasonal and annual variation in the net ecosystem CO_2 exchange of a desert shrub community (Sarcocaulescent) in Baja California, Mexico. Glob Change Biol 11:927–39.

Hutley LB, O'Grady AP, Eamus D. 2001. Monsoonal influences on evapotranspiration of savanna vegetation of northern Australia. Oecologia 126:434–443.

Huxman TE, Turnipseed AA, Sparks JP, Harley PC, Monson RK. 2003. Temperature as a control over ecosystem CO_2 fluxes in a high-elevation, subalpine forest. Oecologia 134:537–46.

Huxman TE, Snyder KA, Tissue D, Leffler AJ, Ogle K, Pockman W, Sandquist DR, Potts DL, Schwinning S. 2004. Precipitation pulses and carbon fluxes in semiarid and arid ecosystems. Oecologia 141:254–68.

Huxman TE, Wilcox BP, Breshears DD, Scott RL, Snyder KA, Small EE, Hultine K, Pockman WT, Jackson RB. 2005. Ecohydrological implications of woody plant encroachment. Ecology 86:308–319.

Jarvis P, Rey A, Petsikos C, Wingate L, tayment M, Pereira J, Banza J, david J, Miglietta F, Borghetti M, Manca G, Valentini R. 2007. Drying and wetting of Mediterranean soils stimulates decomposition and carbon dixide emission: ''Birch effect''. Tree Physiol 27:929–40.

Jenerette GD, Lal R. 2005. Hydrologic sources of carbon cycling uncertainty throughout the terrestrial–aquatic continuum. Glob Change Biol 11:1873–1882.

Konukcu F, Istanbulluoglu A, Kocaman I. 2004. Determination of water content in drying soils: incorporating transition from liquid phase to vapour phase. Aust J Soil Res 42:1–8.

Lauenroth WK, Bradford JB. 2006. Ecohydrology and the partitioning AET between transpiration and evaporation in a semiarid steppe. Ecosystems 9:756–767.

Lai C, Ehleringer JR, Bond BJ, Paw UKT. 2006. Contributions of evaporation, isotopic non-steady state transpiration, and atmospheric mixing on the $\delta^{18}O$ of water vapor in Pacific North west coniferous forest. Plant Cell Environ 29:77–94.

Lee X, Wu H-J, Sigler J, Oishi C, Siccama T. 2004. Rapid and transient response of soil respiration to rain. Glob Change Biol 10:1017–1026.

Loik ME, Breshears DD, Lauenroth WK, Belnap J. 2004. A multi-scale perspective of waterpulse in dryland ecosystems: climatology and ecohydrology of the western USA. Oecologia 141:269–81.

Majoube M. 1971. Fractionnement en oxygene 18 et en deuterium entre l'eau et savapeur. J Chem Phys 58:1423–36.

McLain JET, Martens DA. 2006. Moisture control on trace gas fluxes in semiarid riparian soils. Soil Sci Soc Am J 70:367–77.

Nobel PS. 1999. Physicochemical and environmental plant physiology. San Diego: Academic.

Noy-Meir I. 1985. Desert ecosystems structure and function. In: Evenari M, Noy-Meir E, Goodall DW. Eds. Ecosystems of the world, 12A, Hot deserts and arid shrublands. Amsterdam: Elsevier.

Phillips DL, Gregg JW. 2001. Uncertainty in source partitioning using stable isotopes. Oecologia 127:171–179.

Saetre P, Stark JM. 2005. Microbial dynamics and carbon and nitrogen cycling following re-wetting of soils beneath two semi-arid plant species. Oecologia 142:247–60.

Saleska SR, Miller SD, Matross DM, and others.2003. Carbon in Amazon forest: unexpected seasonal fluxes and disturbance-induced losses. Nature 302:1554–1557.

Scott RL, Watts C, Garatuza J, Edwards E, Goodrich DC, Williams DG, Shuttleworth WJ. 2003. The understory and overstory partitioning of energy and water fluxes in a semi-arid woodland ecosystem. Agric For Meteorol 114:127–39.

Scott RL, Edwards EA, Shuttleworth WJ, Huxman TE, Watts C, Goodrich DC. 2004. Interannual and seasonal variation in fluxes of water and carbon dioxide from a riparian woodland ecosystem. Agric For Meteorol 122:65–84.

Scott RL, Huxman TE, Cable WL, Emmerich WE. 2006. Partitioning evapotranspiration and its relation to carbon dioxide exchange in a Chihuhuan Desert shrubland. Hydrol Process 20:3227–43.

Scott RL, Huxman TE, Williams DG, Goodrich DC. 2006. Ecohydrological impacts of woody-plant encroachment: seasonal patterns of water and carbon dioxide exchange within a semiarid environment. Glob Change Biol 12:311–324.

Shuttleworth WJ. 1993. Evaporation. In Maidment DR Ed., Handbook of Hydrology. New York: McGraw-Hill, pp 4.1–4.53.

Valentini R, Matteucci G, Dolman AJ, and others.2000. Respiration as the main determinant of carbon balance in European forests. Nature 404:861–864.

Weltzin JF, Loik ME, Schwinning S, Williams DG, Fay PA, Haddad BM, Harte J, Huxman TE, Knapp AK, Lin G, Pockman WT, Shaw R, Small E, Smith M, Smith SD, Tissue DT, Zak JC. 2003. Assesing the response of terrestrial ecosystem to potential changes in precipitation. Bioscience 53:941–952.

West AG, Patrickson SJ, Ehleringer JR. 2006. Water extraction times for plant and soil materials used in stable isotope analysis. Rapid Commun Mass Spectrom 20:1317–21.

Williams DG, Scott RL, Huxman TE, Goodrich DC, Lin G. 2006. Sensitivity of riparian ecosystems in arid and semiarid environments to moisture pulses. Hydrol Process 20:3191–3205.

Xu L, Baldocchi DD, Tang J. 2004. How soil moisture, rain pulses, and growth alter the response of ecosystem respiration to temperature. Glob Biogeochem Cycles 18:GB4002 .

Yakir D, Sternberg LSD. 2000. The use of stable isotopes to study ecosystem gas exchange. Oecologia 123:297–311.

Yepez EA, Williams DG, Scott RL, Lin G. 2003. Partitioning overstory and understory evapotranspiration in a semi-arid woodland ecosystem from the isotopic composition of water vapor. Agric For Meteorol 119:53–68.